Correlation of end-of-range damage evolution and transient enhanced diffusion of boron in regrown silicon

L. S. Robertson,[a] M. E. Law, and K. S. Jones
University of Florida, Gainesville, Florida 32611

L. M. Rubin and J. Jackson
Eaton Corporation, Beverly, Massachusetts 01915

P. Chi and D. S. Simons
Chemical Science and Technology Laboratory, National Institute of Standards and Technology, Gaithersburg, Maryland 20899

(Received 9 August 1999; accepted for publication 5 October 1999)

Amorphization of a *n*-type Czochralski wafer was achieved using a series of Si^+ implants of 30 and 120 keV, each at a dose of $1\times10^{15}\,cm^2$. The Si^+ implants produced a 2400 Å deep amorphous layer, which was then implanted with 4 keV $1\times10^{14}/cm^2\,B^+$. Postimplantation anneals were performed in a tube furnace at 750 °C, for times ranging from 15 min to 6 h. Secondary ion mass spectrometry was used to monitor the dopant diffusion after annealing. Transmission electron microscopy (TEM) was used to study the EOR defect evolution. Upon annealing, the boron peak showed no clustering, and TED was observed in the entire boron profile. TEM results show that both {311} defects and dislocation loops were present in the EOR damage region. The majority of the {311} defects dissolved in the interval between 15 min and 2 h. Results indicate that {311} defects release interstitials during the time that boron exhibits TED. These results show that there is a strong correlation between {311} dissolution in the EOR and TED in the regrown silicon layer. Quantitative TEM of dislocation loop growth and {311} dissolution indicates that in addition to {311} defects, submicroscopic sources of interstitials may also exist in the EOR which may contribute to TED. © *1999 American Institute of Physics.* [S0003-6951(99)03848-6]

In order to create a controlled, laterally uniform dopant profile, ion implantation is an integral part of modern integrated circuit (IC) processing. Ion implantation inherently produces a significant amount of damage to the silicon lattice. At sufficiently high doses, an amorphous layer is created on the surface of the silicon wafer. Following ion implantation, a damage layer, termed the end-of-range (EOR) damage region, exists below the amorphous-to-crystalline interface which contains a supersaturation of interstitial point defects[1] created during implantation. During annealing, following solid phase expitaxial regrowth of the amorphous region occurs upon annealing at low temperature (600 °C). At higher temperatures the excess interstitials in the EOR both diffuse away to regions of lower interstitial concentration and precipitate into EOR (type II) extended defects.[2]

It is commonly accepted that excess interstitials in the silicon wafer lead to enhancement of the diffusion rate of dopants such as B, P, and As which diffuse either principally or in part by an interstitialcy mechanism in silicon.[3] Many studies report that during annealing, interstitials from the EOR may induce transient enhanced diffusion (TED) of the dopant contained in the regrown Si layer.[4–6] For nonamorphizing implants it has been reported that {311} defects are a source of interstitials that induce TED.[7] For amorphizing implants the same conclusion has been reported in a more qualitative manner.[8] In this letter, we seek to study in greater detail, the source of interstitials that drive TED during postimplantation annealing of amorphized silicon.

A 150 mm, ⟨100⟩ *n*-type Czochralski silicon wafer was implanted using an Eaton NV-GSD 200.[9] The wafer was first preamorphized using two overlapping Si^+ implantations: 120 keV followed by 30 keV each at a dose of $1\times10^{15}\,cm^2$, in order to create a continuous amorphous layer. The amorphized wafer was then implanted with 4 keV $1\times10^{14}/cm^2\,B^+$. The dose rate of the 120 keV implant was maintained at $0.87\,mA/cm^2$, while the endstation temperature was maintained at 20 ± 1 °C. The tilt/twist angles for each implant were 5°/0°. Postimplantation annealing was performed in a tube furnace at 750 °C in a N_2 ambient. Annealing times ranged from 15 min to 6 h. SIMS profiles were performed on a Cameca IMS-3*f*. The counts of $^{11}B^+$ were obtained using an O_2^+ beam with a net impact energy of 3 keV and 250 nA nominal beam current, rastered over a 250 μm by 250 μm area, with a 60 μm diam detected area. Plan-view TEM of the samples was performed on a JEOL 200CX with images taken in g_{220} weak beam, dark field. Cross-sectional TEM was used to measure the amorphous layer depth. The two main types of defects observed in the TEM were {311} defects and dislocation loops. The concentration of interstitials bound by the EOR extended defects was found using the quantification methodology discussed elsewhere[6] with the addition of a stereographic grid technique to find the areal density of the loops.

The profiles of the implanted boron after annealing at 750 °C are shown as a function of annealing time in Fig. 1. It is evident from the evolution of the profiles that the boron is exhibiting TED for the first 2 h. The correspondence of the profiles annealed for 4 and 6 h indicate that by 4 h the en-

[a]Electronic mail: lancer@grove.ufl.edu

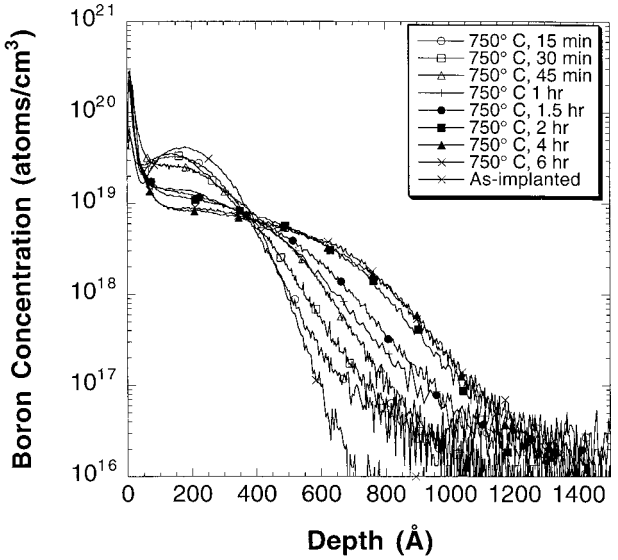

FIG. 1. Boron concentration as a function of annealing time at 750 °C.

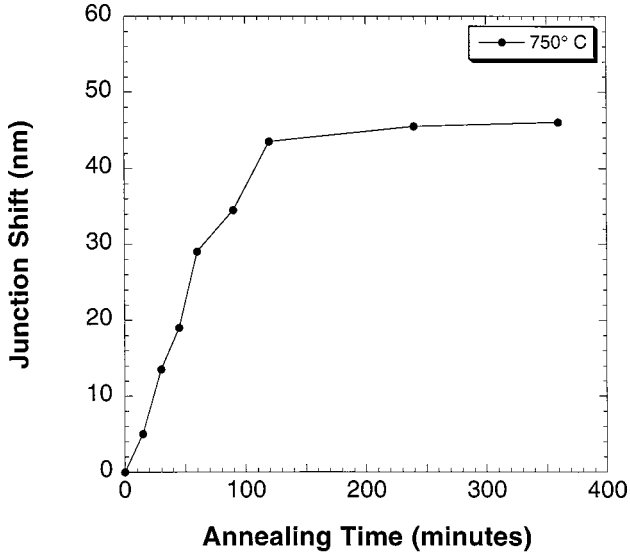

FIG. 2. Junction motion as a function of annealing time at 750 °C.

hancement has decayed to near intrinsic value. The peak of the boron profile shows no clustering although the concentration of the boron is above the clustering limit as observed for nonamorphizing boron implants.[10] The lack of clustering of boron in amorphous layers has been reported previously.[11]

The boron profiles in Fig. 1 indicate that the diffusion characteristics of the tail are anomalous not only in exhibition of enhanced diffusion, but also abnormal distribution. Implant profiles into amorphous solids follow the Pearson-IV distribution and profiles annealed at moderate temperatures and times generally diffuse in a similar distribution. However, the profiles observed for intermediate time intervals at 750 °C in Fig. 1 show an exponential distribution of boron in the diffused tail. The exponential shape of the tail of the boron profiles made it impossible to determine an overall enhancement of the boron in the regrown silicon since the diffusion enhancement varied as a function of depth into the wafer. Therefore, in order to quantify the enhancement of the boron diffusion, the shift in the junction depth of the boron implant was measured at a concentration of $1\times10^{17}/\mathrm{cm}^3$ as shown in Fig. 2. The junction depth increases rapidly as a result of TED through the first 2 h of annealing, then the motion drops back toward the intrinsic diffusion value. After 2 h the junction depth has moved approximately 1000 times further than would be expected by intrinsic diffusion values.[12] The expected junction motion of the initial as-implanted profile in Fig. 1 after a 2 h anneal, is less than 5 nm under intrinsic diffusion conditions due to the boron concentration gradient. During the first 2 h of annealing, the diffusion enhancement is saturated as shown by the constant rate of increase in the junction depth. After 2 h, the TED decays.

The microstructure of the samples was monitored by TEM over the same annealing time interval. The microstructure initially showed a predominance of {311} defects along with small dislocation loops. As the annealing times progressed, the number of {311} defects decreased rapidly and the number of dislocation loops increased slowly. With increasing time the mean size of the {311} defects increased rapidly, while the mean size of the loops grew more slowly. Since interstitial supersaturation induces TED, the number of interstitials bound by both types of defects in the EOR was quantified as a function of annealing time in Fig. 3. Over this annealing interval, the number of interstitials bound by the EOR loops is increasing with annealing time. Between 15 min and 6 h, the number of interstitials bound by the loops increased by $8\times10^{13}/\mathrm{cm}^2\pm1\times10^{13}/\mathrm{cm}^2$. Simultaneous to loop growth, the number of interstitials bound by the {311} defects is decreasing. The number of interstitials released by {311} defects over the annealing interval was $3\times10^{13}/\mathrm{cm}^2\pm1\times10^{13}/\mathrm{cm}^2$. After an initial increase of the dislocation loop density in the first 45 min, the loop density then remained constant through 6 h of annealing. The initial increase in loop density is consistent with some of the {311} defects unfaulting and forming the loops as has been recently reported for nonamorphizing implants.[13] This will be discussed in greater detail in another paper.[14] Over the annealing times studied, the dislocation loops were not in the ''coarsening'' regime, but rather in a growth stage since the density of dislocation loops was constant from 45 min through 6 h and the number of interstitials bound by the loops increased over the same interval. The increase in the number of interstitials bound by the loops was fit with an exponential function of the form $[1-\exp(-t/\tau)]$. The time constant for the saturation of loop growth was found to be approximately 70 min. The {311} defects were unstable over this annealing interval. The dissolution of interstitials from {311} defects was fit with an exponential decay function as shown in Fig. 3. From the decay function, the characteristic time constant for the dissolution of interstitials from {311} defects was found to be approximately 50 min.

In this study, the boron was implanted into an amorphous silicon layer. The interstitials that induce TED originate in the EOR damage region below the initial amorphous-to-crystalline interface. It is apparent that EOR dislocation loops are not contributing to TED over the annealing interval since they are not releasing interstitials, but instead are capturing interstitials. The concentration of interstitials bound by {311} defects decreases by 95% in the first 2 h of annealing. The diffusion enhancement of the boron decays after 2 h

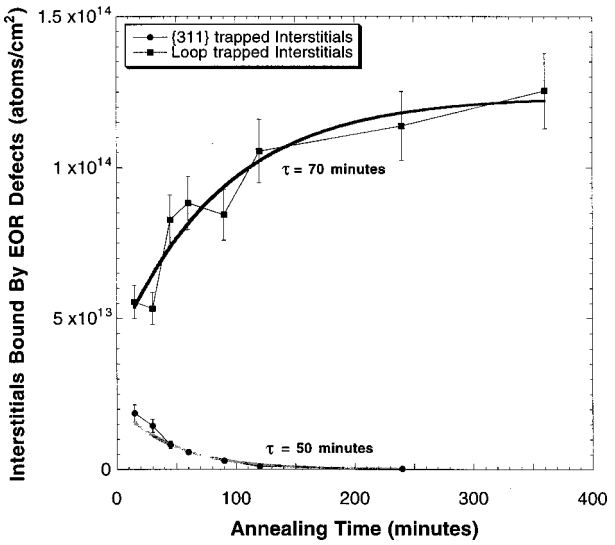

FIG. 3. Density of interstitials bound by EOR defects as a function of annealing time at 750 °C.

of annealing. Thus, there is a correspondence of the time to dissolve {311} defects and the time over which TED decays to an intrinsic value. This shows that {311} defects are releasing interstitials during TED and are no longer present after TED has decayed.

Despite this evidence, the theory that {311} defects are the most significant source of interstitials that induce TED in the regrown region of the silicon remains in question. This study cannot confirm or disprove this theory due to several uncertainties. Of these uncertainties, the most significant are whether submicroscopic interstitial clusters (SMICs) exist, the number of interstitials needed to induce TED, and whether interstitials released by {311} defects leave the EOR or are incorporated into dislocation loops in the EOR. Resolution of the latter two uncertainties is beyond the scope of this discussion. Concerning the existence of SMICs, the authors contend that they do exist. Evidence for this is the inability to account for the growth of the dislocation loops in the EOR by considering only the interstitials released by {311} defects since the dislocation loops grew by 8×10^{13} interstitials/cm^2, and the number of interstitials released by dissolving {311} defects was 3×10^{13}/cm^2. Additional evidence is the similarity of the time constants for loop growth and {311} dissolution, indicating that the same phenomena controls both processes. The smallest {311} defect that is routinely observable by TEM would contain approximately 100 interstitials. There are two general possibilities. The first is that all excess interstitials (not in dislocation loops) exist in visible {311} defects and there are very few interstitial defects in the lower end of the size distribution of interstitial clusters. The second possibility is that the peak of the distribution of interstitial cluster distribution is below the resolution limit of the microscope (sub 100 atoms) and the {311} defects observed are just the tail of the higher end of the size distribution. The observation of growth in the interstitial content in the loops in excess of the interstitial content of the {311} defects suggests that the second possibility may be correct.

At present, the EOR damaged region is probably best viewed as a ''leaky box,'' containing interstitials in an undetermined number of configurations undergoing conservative and nonconservative point defect reactions. The nonconservative reactions release interstitials which induce TED. For amorphizing implants {311} defects in the EOR serve as a useful indicator of interstitial supersaturation and therefore TED because of the correlation of the timescales of {311} dissolution and TED. This correlation does not denote causation nor does it deny the existence of SMICs.

In conclusion, upon annealing, excess interstitials in the EOR damaged region of amorphized silicon precipitate into {311} defects, dislocation loops, and possibly SMICs. At 750 °C, as the annealing time increases, the {311} defects dissolve releasing interstitials into the EOR damage region. At the same time that {311} defects release interstitials, the boron in the regrown silicon exhibits TED. The correspondence of the time to release interstitials from {311} defects and the decay of TED in the regrown silicon supports the theory that interstitials from {311} defects are contributing to the interstitial supersaturation that causes TED. Dislocation loops are not releasing interstitials over the annealing interval studied but in fact are growing in both density and interstitial content. The increase in interstitial density in the loops cannot be explained quantitatively by interstitial release from the {311}s and this strongly suggests the existance of SMICs since no other defects are visible by TEM. In addition, these SMICs which may in theory be the principle source of TED must dissolve and release interstitials over approximately the same time interval as the {311} defects.

[1] M. Servidori, Nucl. Instrum. Methods Phys. Res. B **19/20**, 443 (1987).
[2] K. S. Jones, S. Prussin, and E. R. Weber, Appl. Phys. A: Mater. Sci. Process. **45**, 1 (1988).
[3] P. M. Fahey, P. B. Griffin, and J. D. Plummer, Rev. Mod. Phys. **61**, 289 (1989).
[4] R. Angelucci, P. Negrini, and S. Solmi, Appl. Phys. Lett. **49**, 1468 (1986).
[5] L. S. Robertson, K. S. Jones, A. Lilak, M. E. Law, P. S. Kringhoj, L. M. Rubin, J. Jackson, D. S. Simons, and P. Chi, Appl. Phys. Lett. **71**, 3105 (1997).
[6] K. S. Jones, M. K. J. Chen, M. Puga-Lambers, B. Freer, J. Berstein, and L. Rubin, J. Appl. Phys. **81**, 6051 (1997).
[7] D. J. Eaglesham, P. A. Stolk, H.-J. Gossmann, and J. M. Poate, Appl. Phys. Lett. **65**, 2305 (1994).
[8] K. S. Jones, L. H. Zhang, V. Krishnamoorthy, M. Law, D. S. Simons, P. H. Chi, L. Rubin, and R. G. Elliman, Appl. Phys. Lett. **68**, 2672 (1996).
[9] Certain commercial equipment, instruments, or materials are identified in this letter to specify adequately the experimental procedure. Such identification does not imply recommendation or endorsement by the National Institute of Standards and Technology, nor does it imply that the material or equipment identified are necessarily the best available for the purpose.
[10] P. A. Stolk, H.-J. Gossmann, D. J. Eaglesham, D. C. Jacobson, J. M. Poate, and H. S. Luftman, Appl. Phys. Lett. **66**, 568 (1995).
[11] K. S. Jones, R. G. Elliman, M. Petravic, and P. Kringhøj, Appl. Phys. Lett. **68**, 3111 (1996).
[12] R. B. Fair, in *Impurity Doping Processes in Silicon*, edited by F. F. Y. Wang (North Holland, Amsterdam, 1981), p. 315.
[13] J.-H. Li and K. S. Jones, Appl. Phys. Lett. **73**, 3748 (1998).
[14] L. S. Robertson and K. S. Jones (unpublished).